PERGAMON

International Journal of Multiphase Flow 26 (2000) 1351–1368

International Journal of Multiphase Flow

www.elsevier.com/locate/ijmulflow

Experimental study on nucleate boiling enhancement and bubble dynamic behavior in saturated pool boiling using a nonuniform dc electric field

Y.C. Kweon [a,*], M.H. Kim [b]

[a] *Division of Mechanical and Control Engineering, Sun Moon University, 100 Kalsanri, Tangjeong Myeon, Asansi, Chung nam, 336-840, South Korea*

[b] *Department of Mechanical Engineering, Pohang University of Science and Technology, San 31, Hyoja Dong, Nam-gu, Pohang, 790-784, South Korea*

Received 27 March 1998; received in revised form 21 July 1999

Abstract

In order to investigate the effects of an electric field on the nucleate boiling heat transfer enhancement including bubble dynamic behavior, basic experiments have been performed under saturated pool boiling. In the present study, the working fluid is Freon-113 and the plate-wire electrode is used to generate a steep electric field gradient around the wire. A single-photo/high photography method is applied to measure boiling parameters. The experimental results show the shift of the boiling curve and the delay of ONB and CHF to a higher heat flux by an electric field. These EHD effects are much more considerable when the applied voltage increases. It is confirmed that the mechanisms of EHD nucleate boiling are closely connected with the dynamic behaviors of bubbles. Boiling parameters are investigated by using a high speed camera. The present results show that the boiling parameters are significantly changed by the electric field strength and nonuniformity. The relative contribution of latent heat to boiling heat transfer in an electric field is introduced. At very high voltage, the amount of latent heat transported by bubbles nearly corresponds to the total heat flux.

Keywords: Electrohydrodynamics; Electric field; Nucleate boiling; Heat transfer enhancement; Bubble; Dynamic behavior

* Corresponding author.
E-mail addresses: yckweon1@omega.sunmoon.ac.kr (Y.C. Kweon), mhkim@vision.postech.ac.kr (M.H. Kim).

0301-9322/00/$ - see front matter
PII: S0301-9322(99)00090-7

1. Introduction

The enhancement of boiling heat transfer is very important to many industries including engineering and power plant. Among them, the studies on nucleate boiling heat transfer have received a great deal of attention from many researchers. In recent years, the importance of electrohydrodynamic (EHD) enhancement of heat transfer on the boiling process has been widely recognized. Especially it has been known that the nonuniform electric field considerably enhances the rate of nucleate boiling heat transfer of several refrigerants (CFC, HCFC).

A number of experimental and analytical efforts have been devoted to obtain more information about EHD effects (Jones, 1978; Yabe and Maki, 1988; Kawahira et al., 1990; Ogata et al., 1992; Seyed-Yagoobi et al., 1996). Some major effects of an electric field on boiling include the increase of maximum heat flux and bubble frequency and the decrease of bubble size. In particular, these effects are more remarkable when the electric field is strong and nonuniform due to the mutual interactions between a bulk liquid, vapor bubbles and an electric field. The EHD phenomena depend on the electric parameters, the fluid parameters and the geometry and arrangement of electrodes to produce the strong nonuniform electric field. Because of the complexity of the EHD phenomena involved, however, great efforts on the EHD boiling process have been made to study the fundamental mechanisms of EHD boiling heat transfer (Lovenguth, 1968; Jones, 1978; Cooper, 1990; Damianidis et al., 1992; Kweon et al., 1996). It has been found from these studies that more bubbles of small size depart at the heated surface by a nonuniform electric field and these bubbles enhance the heat transfer. Since the above macroscopic study is far from being satisfactory, however, the behavior of a single bubble attached to a heated wall in electric fields have been performed by Ogata and Yabe (1993); Cho et al. (1996; 1998) and Kweon et al. (1998). They analyzed bubble behavior and the electric forces on a bubble. It has been reported that the bubble deformation significantly depended on the nonuniformity of an electric field.

Although the electric field can affect the bubble dynamics considerably, however, the basic studies on the EHD bubble dynamics are few. Moreover, no electrohydrodynamically-general theory exists yet concerning the relationship between nucleate boiling heat transfer and the boiling dynamics in a nonuniform electric field. Particularly, the effects of an electric field on the nucleate boiling heat transfer enhancement can be well explained in terms of bubble behaviors. Since the information about bubble dynamics is not well understood, however, detailed knowledge of bubble behaviors is necessary to clarify the basic mechanisms of the EHD boiling process.

In this study, basic experiments have been performed to investigate the effects of an electric field on the nucleate boiling heat transfer enhancement including the dynamic behaviors of bubbles. For this purpose, the boiling curve, onset of nucleate boiling and critical heat flux are measured. Bubbles in the EHD nucleate pool boiling are also visualized to provide the explanations on the EHD effect. The relevance of this work to the EHD boiling process is found from the fact that the effects of an electric field on bubble behaviors can be explained by examining bubble parameters (the nucleation site, the bubble velocity, frequency and departure size). These are used to determine how the relative latent heat contribution is changed by an

electric field. Although the EHD phenomena addressed in this paper are not sufficient to describe the nucleate boiling heat transfer enhancement, the present results may provide an initial perspective on the effects of the electric field on bubble dynamics.

2. Experimental arrangements

2.1. Experimental facility

A schematic diagram of the EHD pool boiling apparatus is shown in Fig. 1. The boiling apparatus consists of a boiling vessel, a condenser, an electrode system, a 30 kV–2 mA dc high voltage power supply, a variable dc controller and a high voltage probe.

The boiling vessel is insulated and made of tempered glass to facilitate visual observations. The condenser located above the boiling vessel is provided for condensing the vapor generated in the vessel. The high voltage probe is used to measure accurately the positive dc voltage applied to the upper electrode, while the lower electrode is grounded. The electrode system is a plate-wire electrode, consisting of an upper plate electrode (copper, 110×85 mm) and a lower wire electrode (platinum, diameter 0.37 mm and length 140 mm). The edge of the upper plate electrode is rounded to avoid disturbance of the electric field. The electrode gap is 16 mm. In the present experiment, a thin wire is selected in order to produce a large gradient of the electric field at the surface of the wire. It generates the strong nonuniform electric field.

The boiling experiments are carried out by cleaning thoroughly the boiling chamber with distilled water and rinsing repeatedly. The platinum wire and electrode assembly are first soaked in acetone and then dried before assembling. In the present study, Freon-113

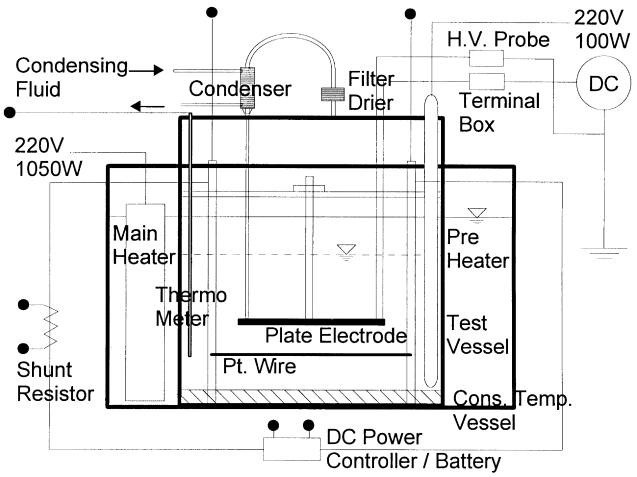

Fig. 1. Schematic diagram of EHD pool boiling apparatus.

is used as the working fluid. It has well-established properties (ASHRAE, 1993) and has a relatively high boiling point and is compatible with a wide array of common materials (however, Freon-113 has been regulated due to its high ozone depletion and global warming effect). Before each experiment, Freon-113 is heated by using a 1050 W main heater and a 100 W adjustable electric pre-heater. After being sufficiently preheated for about 2 h, it is degassed.

In order to determine the wire temperature by Joule heating, an electrical resistance direct heating method is used. The heat flux is calculated from the power given to the wire. The platinum wire used as a resistance heater and a resistance thermometer is electrically heated by two 12 V batteries. The voltage and the current are measured during each experiment to determine the change in the wire resistance. The liquid temperature is maintained at 46.3°C, so that heat losses between the apparatus and the surroundings would be nearly constant in all runs and measured by two calibrated K-type sheathed thermocouples placed 10 mm from the side of a wire. All experiments are made at atmospheric pressure.

The most important liquid properties affecting the EHD phenomena are electric conductivity and the permittivity. The brief review on these two electric properties has been presented by Turnbull (1968). Electric conductivity has a much larger variation with temperature (about 5%/°C) compared with that of the permittivities (about 0.1%/°C). Thus, for a single-phase case, the EHD effects are depended on the inhomogeneous distribution of the electric conductivity. In this case, the electrophoretic force (Coulomb force) becomes predominant. For the two-phase boiling case including nucleate boiling, the induced charges can be produced on a bubble-liquid interface. The charges accumulated on the bubble-liquid interface depend on the electric charge relaxation time and bubbling. If bubbling is much less than the electric charge relaxation time, the accumulation of the charges is negligible on the bubble-liquid interface. In this case, the dielectrophoretic force due to the different permittivities between the liquid and gas phases becomes predominant. The electric charge relaxation time of Freon-113 is about 10 s. The time of bubbling is of the order of several 10 ms. Thus, the effect of the electric field on bubble behaviors in pool boiling of Freon-113 can be explained by the dielectrophoretic force. In addition, since the conductivity of Freon-113 is very poor, the electric current through Freon-113 is negligible (the current measured in this study is of the order of μA).

Each experiment is carried out with varying applied voltage (up to 20 kV). And it is maintained under steady-state conditions (within ±0.5% the setting voltage), and then increased to the next step. Before each experiment, the reference conditions in the zero electric field have been confirmed. During an experiment, the pool temperature is nearly constant within a range of ±0.1°C. Reproducibility of the experimental data is examined by conducting experiments under the same operating conditions at different times. The data are found reproducible. The method of Moffat (1985); Wang and Simon (1988) is used to determine the uncertainties on wire temperature, liquid temperature, heat flux and heat transfer coefficient. The sources of estimation of uncertainties in the present study are mostly either instrument specification or deviation estimated from the experiments. The uncertainty on the voltage is estimated as 17.44 mV and the uncertainty of the wire resistance is estimated as 0.0347Ω. The uncertainties on the wire length and diameter are estimated as ±0.5 mm and ±0.002 mm,

respectively. In nucleate boiling, the resulting uncertainties are below $\pm 0.4^{\circ}C$ for the wire temperature and liquid temperature, and within $\pm 5\%$ for the heat flux, and within $\pm 9\%$ for the heat transfer coefficient.

2.2. Visual observation

The high photographic equipment is set up (NAC E-10 16 mm camera) to examine the effects of an electric field on the dynamic behaviors of bubbles in pool boiling. It is capable of a frame rate up to 10,000 fps. The frame rate is regulated within $\pm 1\%$. In order to understand bubble dynamics in the nonuniform electric field, 50 frames recorded at 5000 fps are used. The EHD effects on bubble departure at a heated wire in a saturated boiling are photographed at 240 kW/m^2. For close-up photography, a close-up adapter is available, which is a combined focal length lens of 100 mm with extension tubes. For each frame, a relative size scale is obtained by measuring the projected wire diameter and then comparing it with the actual wire diameter. All data are obtained by counting bubbles within the measurement area (30 by 15 mm) for the field of view shown in Fig. 2.

3. Results and discussions

3.1. Electric field distribution

The electric field distribution around a wire immersed in a dielectric liquid is obtained by using an electric potential. If the wire is thin, practically the whole electric potential is concentrated within a short distance from the surface of the wire. Using an electrical image method (Kraus, 1992), the electric potential distribution of a wire can be obtained by

$$(x-a)^2 + y^2 = r^2, \tag{1}$$

where, a is the x coordinate of circle center $(=l(K^2+1)/(K^2-1))$, r is the equipotential radius $(=2lK/(K^2-1))$ and $K = \sqrt{(x+l)^2+y^2} \Big/ \sqrt{(x-l)^2+y^2}$.

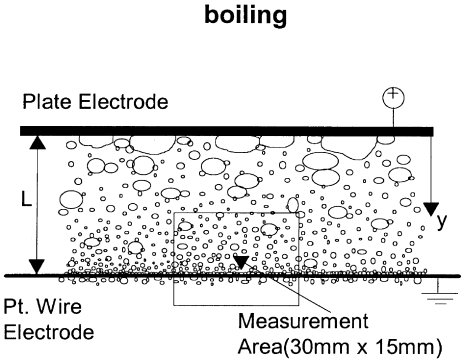

Fig. 2. Cross section of the plate-wire electrode for nucleate pool boiling.

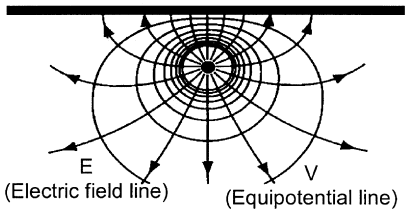

Fig. 3. Distribution of equipotential lines (indicated by circles) and electric field lines (indicated by arrows) around a wire.

Figure 3 shows equipotential lines (indicated by circles) and the electric field lines (indicated by arrows) around the wire. The electric field is perpendicular to the equipotential line. Due to the electric field concentration, the electric potential in the vicinity of the wire becomes stronger and its electric field is more nonuniform compared with that of the upper plate region. The electric field is asymmetric around the wire and is the strongest where the wire faces the plate electrode.

Figure 4 shows that the y-directional normalized electric field strength. Here E_o is the uniform electric field strength (=applied voltage V/electrode gap L). The y-directional electric field strength E_y around the wire can be given by

$$E_y = \frac{2V\sqrt{l^2 - R_w^2}}{(l^2 - R_w^2 - y^2)ln[(l + \sqrt{l^2 - R_w^2})/R_w]}, \tag{2}$$

where l, R_w and y are the distance between a plate and the center of a wire, the wire radius and the axis of coordinate. Detail analysis of the electric effects on the practical nucleate boiling with high heat flux conditions is difficult because the local field strengths and electric charges are themselves affected by the complex behaviors of bubbles (as illustrated in Fig. 8).

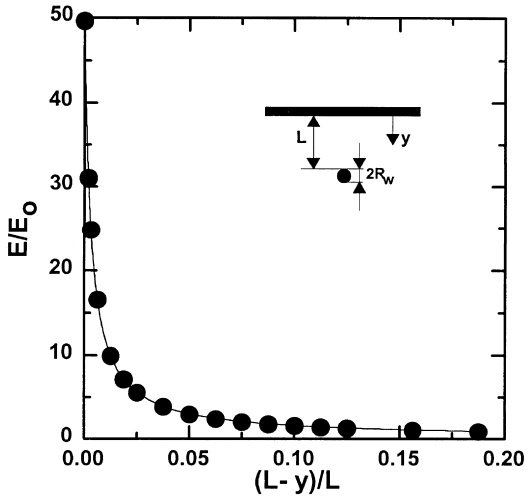

Fig. 4. Electric field strength around a wire.

In the present analysis, no bulk free charges and bubbles in a dielectric liquid are assumed. The electric field distribution is determined solving the Laplace equation. Equation (2) indicates that the electric field strength increases with increasing the applied voltage. As expected in Fig. 3, the electric field is concentrated near the wire and its distribution is also inhomogeneous. Especially, at the wire surface ($y = L$), the magnitude of the electric field is about 50 times greater than that of the uniform electric field strength. This means that bubbles may experience much larger electric forces due to the strong nonuniform electric field.

Considering Helmholtz free energy (Panofsky and Phillips, 1962), an electrical force density f_e can be generally expressed by

$$f_e = \rho_c E - \frac{1}{2}E^2\nabla\varepsilon + \frac{1}{2}\nabla\left(\rho E^2\left(\frac{\partial\varepsilon}{\partial\rho}\right)_T\right) \tag{3}$$

where ρ_c, E, ε and ρ are the free charge density, the electric field strength, the permittivity and the liquid density. The physical meanings of each term have been introduced in detail by Melcher (1981). The first term is the Coulomb force exerted on the net free charges or ions. The second term is the force produced by the spatial change of permittivity. The third term is the force caused by the nonuniformity of the electric field. The second and third terms represent the force exerted on dielectric materials. These two terms become important in the case of EHD phenomena in liquids as well as the gas-liquid interface. Since no appreciable free charges are generated in a liquid used in the present study, the Coulomb force effect is minimal. Thus, second and third terms will play the major role for the discussion in this study.

In the case of the nonuniform electric field, since the net electric force exerted on bubbles is proportional to the square of the gradient of the electric field strength, it becomes much more significant when the electric field is nonuniform and its intensity is strong. As will be shown later, the departure behaviors of bubbles is more noticeable at the vicinity of the wire as the electric field increases. In order to add EHD effects to the thermal-hydraulic phenomena, we should design the electrode configuration to effectively use the field nonuniformity.

3.2. Boiling heat transfer enhancement

3.2.1. EHD effects on boiling heat transfer

The rate of heat transfer of a wire Q_w is defined by

$$Q_w = \Delta V_w \times i_w, \tag{4}$$

where ΔV_w and i_w are the voltage drop and the current.

The heat flux of the wire q_w'' can be given by

$$q_w'' = \frac{Q_w}{\pi D_w L_w} \quad \text{or} \quad q_w'' = h\Delta T, \tag{5}$$

where D_w is the wire diameter, L_w is the wire length, h is the heat transfer coefficient and ΔT is the difference between the wire temperature (T_w) and the bulk liquid temperature (T_{sat}).

In order to understand the EHD effects on saturated pool boiling, the trend of the boiling

curve versus an applied voltage is investigated at five different heat fluxes, 29 kW/m^2 (low nucleate boiling, LNB), 69, 115 and 183 kW/m^2 (moderate nucleate boiling, MNB), and 265 kW/m^2 (high nucleate boiling, HNB). Fig. 5 shows the pool boiling curves under 5, 10 and 15 kV dc voltages, compared with that under the zero field case. With increasing the applied voltage, the boiling curves are shifted to lower wire temperature and the increase of heat flux is remarkable. When the wire temperature is about 75°C, the heat flux at 15 kV dc voltage increases about 3.5 times greater than that at the zero field case.

The effects of an electric field also increase the heat transfer coefficient. Under the present experimental conditions, it is found that the relative heat transfer coefficients (the influence of electric field on the heat transfer coefficient ratio) is nearly proportioned to the magnitude of the applied voltage. For a given heat flux, the relative heat transfer coefficient increases with increasing the applied voltage. At 15 kV dc voltage, the heat transfer coefficient is enhanced about 215% for 29 kW/m^2, 127% for 69 kW/m^2, 81% for 115 kW/m^2, 54% for 183 kW/m^2 and 32% for 265 kW/m^2. This shows that the sensitivity of nucleate boiling heat transfer to an electric field is more effective at lower heat fluxes.

3.2.2. Onset of nucleate boiling and critical heat flux

The electric field also affects onset of nucleate boiling (ONB) and critical heat flux (CHF). In order to determine ONB and CHF, the steady-state experiment has been carried out. ONB is defined as the heat flux measured at the moment of bubble generation on the wire. CHF is defined as the heat flux caused by the onset of film boiling, which is validated by the drastic increase in the wire temperature. Fig. 6 shows the effects of an electric field on ONB and CHF. ONB and CHF undergo a larger increase by applying a high voltage. At 7.5 kV dc voltage, ONB and CHF increase about 450 and 80%, respectively, compared with that at the zero field case. Thus, the electric field delays ONB and CHF. CHF measured from the present study are

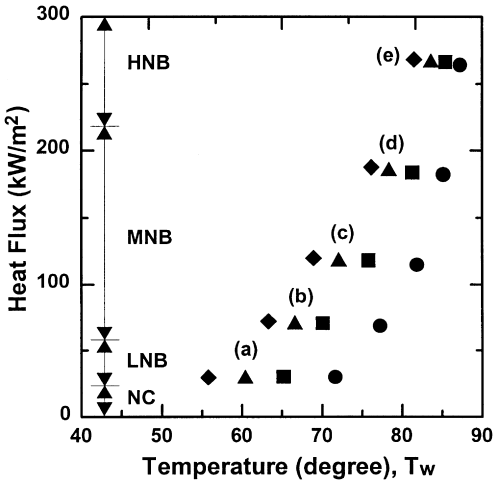

Fig. 5. EHD pool boiling curves of a wire in a nonuniform dc electric field: (a) 29 kW/m^2; (b) 69 kW/m^2; (c) 115 kW/m^2; (d) 183 kW/m^2; (e) 265 kW/m^2 (●: 0 kV, ■: 5 kV, ▲: 10 kV, ◆ 15 kV).

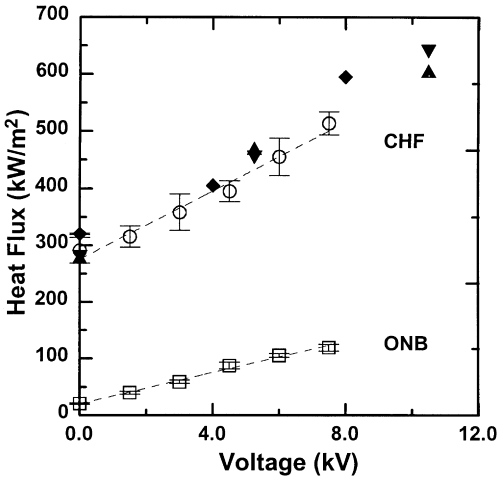

Fig. 6. Onset of nucleate boiling and critical heat flux in a nonuniform dc electric field (ONB: □ present data; CHF: ○ present data, ▲ Choi, 1962, ▼ Lovenguth, 1968, ◆ Carrica et al., 1995).

in good agreement with the previous works (Choi, 1962; Lovenguth, 1968; Carrica et al., 1995). The effect of an electric field of enhanced ONB and CHF may be explained as follows.

As a nonuniform electric field is applied, an electroconvective flow is generated around the wire. As described previously, the electrical conductivity of liquid is dependent on temperature. Due to a large gradient of temperature field at the surface of the heated wire, the electric charges are induced within the thermal layer. The movement of these charges produces the electroconvective flow. The present study shows that the electroconvective flow plays a role to determine ONB heat flux. The flow velocity is faster with increasing the applied voltage (up to below 5 kV), and then the velocity of the EHD flow is supposed to increases almost linearly. At about 5 kV dc voltage, the EHD flow becomes gradually disturbed. At above 9 kV dc voltage, the flow field becomes turbulent. From these, we can see that the effect of an electric field on electroconvective flow is divided into three flow regimes along with the magnitude of a given applied voltage.

The effects of an electric field on the departure behaviors of bubbles in a pool are

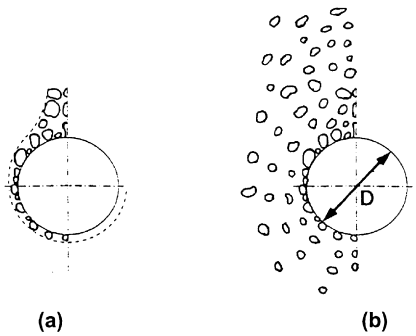

Fig. 7. Dynamic departure behavior of bubbles around a wire; (a) zero field, (b) electric field.

conceptually shown in Fig. 7. The figure describes that the imposing nonuniform electric field can change bubble dynamics. Although the increase of CHF is caused by both the electroconvection effect and the EHD boiling effect due to bubble behaviors, the EHD boiling effect by bubble behaviors becomes more important as the applied voltage increases (see Fig. 14). In the nonuniform electric field, EHD boiling effect can be explained by considering an electric force. The electric force F_e acting on a bubble can be given by (Pohl, 1958)

$$\bar{F}_e = 2\pi R_b^3 \varepsilon_o \frac{1-\varepsilon_r}{1+2\varepsilon_r} \nabla E^2, \tag{6}$$

where R_b is the equivalent bubble radius, ε_o is the permittivity of a vacuum, ε_r is the relative permittivity and E is the electric field strength.

This force is due to the combined effect of the different permittivities of liquid and vapor and the nonuniformity of the electric field. It is experimentally evidenced that a number of small bubbles move far from a wire (Fig. 8). The active motion of these bubbles leads to the higher heat transfer coefficient due to the enhanced latent heat and mixing effect by bubbles departing from the heated wire. From this, we can see that CHF under boiling conditions becomes significantly enhanced by an electric field, hence the transitions to burnout become prevented.

3.2.3. Bubble observations

Fig. 8 shows the instantaneous behaviors of bubbles in EHD nucleate pool boiling at 240 kW/m^2. With increasing electric field strength from zero, visual observations indicate that the electric field modifies the bubble dynamics of the boiling process. In the absence of the electric field (Fig. 8(a)), bubble behaviors are seen to be extremely chaotic. Bubbles are gathering together on the upper part of the wire, coalescing with other bubbles and, finally, departing from the wire. At below 1 kV, no appreciable effects of an electric field on bubble behaviors are observed. At above 2 kV, bubble behaviors are gradually modified, such as the bubble departure frequency and size. At above 5 kV (Fig. 8(b–e)), the dispersion of bubbles becomes more noticeable. The bubbles are organized in more ordered columns with smaller diameters and higher departure frequencies, with reduced coalescence.

It is also observed that the bubbles generated at the lower side of a wire move side-downward due to the electric force. The direction of the electric force acting on bubbles is the electric field line, as shown in Fig. 3. The modified bubble dynamics can be explained by comparing the direction of the electric force with that of the buoyancy force. For the upper part of the wire, since the electric force is directed side-upward, the resultant force acts as the additive effect of the buoyancy force. For the lower part of the wire except its bottom, it is directed side-downward. When the electric force is smaller than the buoyancy, bubbles slide up along with the surface due to the direction of the resultant force.

The bubble rising time at the finite depth as our experimental conditions is much smaller than the electric relaxation time. In this case, the dielectrophoretic force becomes very important, as mentioned before. This force attracts bubbles toward the region of weaker electric field. That is, it tends to pull bubbles off from the heated wire more rapidly. With

increasing the applied voltage and the nonuniformity of the electric field, the dielectrophoretic force increases. Thus, many bubbles with small size depart rapidly away from the wire before they grow sufficiently, as we can see from Fig. 11. From the above considerations, we can see that the electric field affects the bubble production rate and the bubble dynamics.

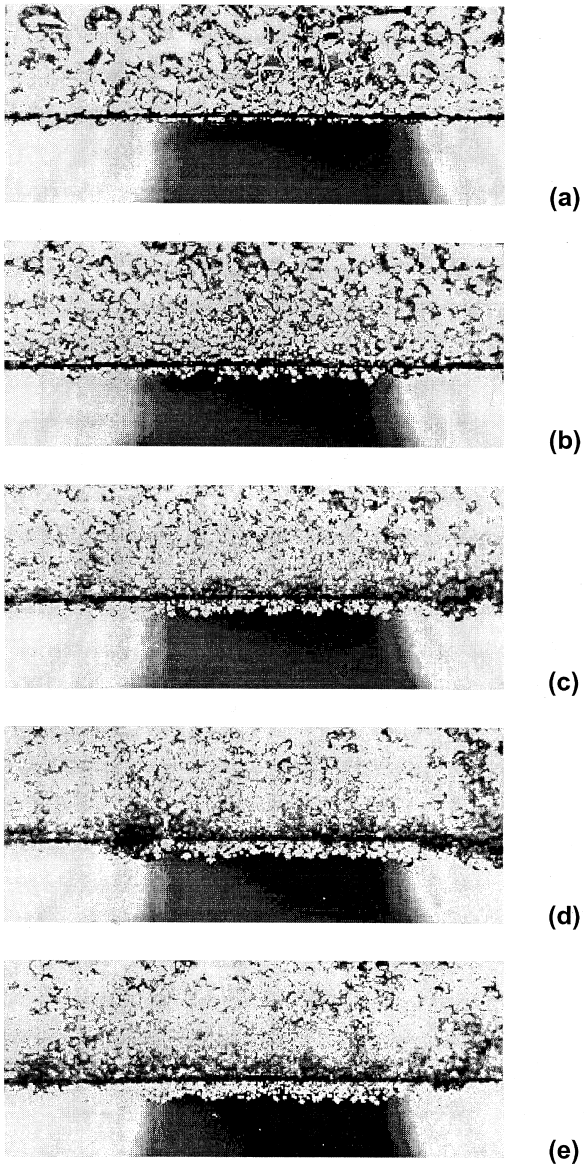

Fig. 8. Photographs of EHD nucleate pool boiling in a nonuniform dc electric field at 240 kW/m^2; (a) 0 kV, (b) 5 kV, (c) 10 kV, (d) 15 kV, (e) 20 kV.

3.3. Dynamics of bubbles in an electric field

3.3.1. Nucleation site density

The determination of the nucleation site density in a nonuniform electric field is subjective. It is difficult to determine exactly how many sites are active since some sites are very close to each other. A best guess is made concerning the average number locations from which bubbles generate. When analyzing successive frames on the slow-motion film, nucleation sites are considered active as soon as bubbles appear at a heated wire. Most parts of the wire have nucleation sites, which are almost always active, whereas some parts have sites which are sporadically active. Fig. 9 shows the average density of active nucleation sites as a function of the applied voltage. The figure indicates that the active nucleation site density increases with increasing the applied voltage. From the result, it is supposed that the effects of the nonuniform electric field may activate the nucleation sites of the wire. The uncertainties estimated for the number density of active nucleation sites are within about $\pm 8\%$.

Although it is suggested that the nucleation site density is also closely related to the cavity sizes on the wire, the relationship between the nucleation site density and cavity size is not introduced in the present study because the sizes of nucleation sites are too small for direct measurement. Thus, detailed studies on the bubble generation at cavities in a nonuniform electric field will be done.

3.3.2. Bubble velocity

Bubble velocity is also affected by a nonuniform electric field. In order to determine the bubble velocity, we use a time marking function of the high-speed camera. The movement of bubbles recorded on the film is traced by a frame-by-frame analysis. In the present study, only the vertical velocity component of bubbles is considered because it is difficult to measure the radial velocity component of bubbles. Fig. 10 shows the average bubble velocities as a function of the applied voltage. The uncertainties estimated for bubble velocity are within about $\pm 7\%$.

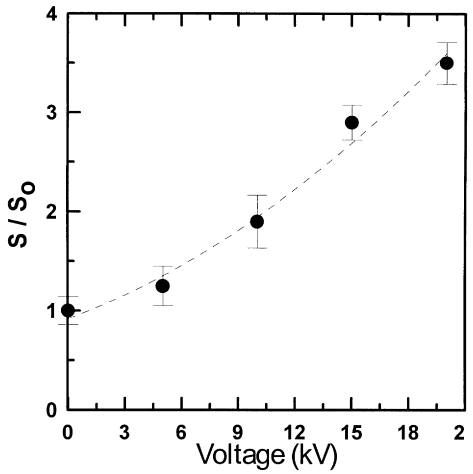

Fig. 9. Average number density of active nucleation sites in a nonuniform dc electric field.

At 20 kV dc voltage, the average bubble velocity increases about 5 times greater than that of zero field case, despite the decrease in bubble size. The velocities of bubbles departing on the wire are faster than bubbles in a bulk liquid due to the strong electric field concentration near the wire. It is found that bubble departure away from the lower side of the wire is stopped at a certain distance and the departure distance increases with increasing the applied voltage. From this, we can see that a liquid region where the resultant forces acting on a bubble is zero can be expected. It is also noted that the electric force is very strong due to the steep electric gradients close to the wire. When the electric force exceeds gravity, bubbles can be easily removed even from the downward facing region of the wire.

3.3.3. Bubble frequency

When bubbles start to grow on a heated wire, the growth time is required to depart from the wire. After departed, cold liquid then rushes in behind the departing bubbles and touches the heated wire. A waiting time is required to heat the new liquid layer so that nucleation can occur. In this case, the growth time represents the time of departure and the waiting time represents the time of liquid contact. The average bubble frequency f is then defined by

$$f = \frac{1}{n} \sum \frac{1}{t_w + t_g}, \tag{7}$$

where n, t_w and t_g are the bubble number, the average waiting time and the average growth time.

Figure 11 shows the average bubble frequencies and the average waiting and growth times as a function of the applied voltage. The uncertainties for bubble frequency are estimated to be within about $\pm 11\%$. The average waiting and growth times of bubbles are obtained by counting bubbles leaving sites over the duration of successive frames. The bubble frequency is highly site-dependent for a given applied voltage. The figure shows that the average waiting and growth times decrease with increasing applied voltage. It is also found that the waiting time is larger than the growth time. At 20 kV dc voltage, the average bubble frequency increases about 14 times greater than that of zero field case. As the result, the bubble size may

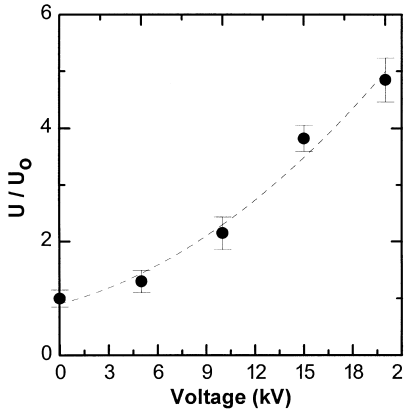

Fig. 10. Average bubble velocity in a nonuniform dc electric field.

decrease. From the figure, we can see that the bubble departure cycle is drastically changed by the effects of the nonuniform electric field.

3.3.4. Bubble diameter

Based on bubble observations, we can see that the bubble shape is slightly irregular. Bubbles observed are transferred into an equivalent area because the bubble volume can be determined from a two-dimensional image. An equivalent bubble diameter is calculated from the average volume of bubbles. Then, the equivalent spherical bubble diameters can be determined by

$$V_b = \tfrac{4}{3}\pi a_b^2 b_b = \tfrac{1}{6}\pi D^3, \tag{8}$$

where V_b, a_b, b_b and D the bubble volume, the bubble major axis, the bubble minor axis and the equivalent bubble diameter.

In the nonuniform electric field, the bubble diameter at the moment of detachment can be predicted by using the electric force which serves as a driving force. By considering a steady-state force balance between buoyancy, surface tension and electric force acting on a bubble, the bubble diameter D can be expressed by

$$D = C_1\left(\frac{6\gamma \sin^2\theta}{\Delta\rho g K_e}\right)^{1/2} \tag{9}$$

where γ is the surface tension, θ is the contact angle, ρ is the density, g is the gravitational acceleration and $K_e = 1 + C_2(\varepsilon_r\varepsilon_o/\Delta\rho g)[(1-\varepsilon_r)/(1+2\varepsilon_r)]\nabla E^2$. In deriving Eq. (9), it is assumed that (1) bubbles are unaffected by the inertial force, (2) the surface tension and the contact angle are unaffected by an electric field and (3) no electric charges exist on a vapor-liquid interface. The constant C_1 is determined from the experiments under the zero electric field conditions and C_2 is best-fitted from the data on bubble diameters in an electric field. The proposed values of empirical constants C_1 and C_2 are 0.7 and -0.01 and these values are

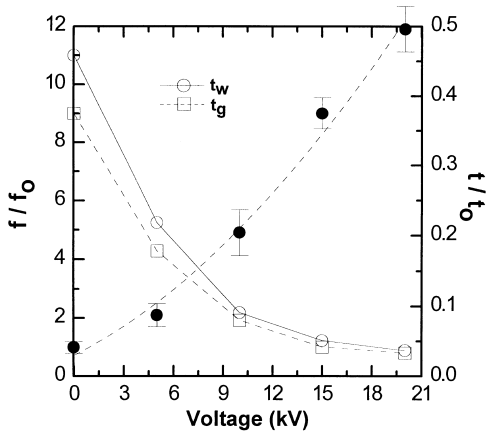

Fig. 11. Average bubble frequency (●), average waiting time (○) and average growth time (□) in a nonuniform dc electric field.

expected to be used for evaluating the bubble diameter at the moment of detachment in the nonuniform electric field. E in Eq. (9) means the electric field strength in the absence of bubbles.

Figure 12 shows the average bubble diameter in the nonuniform dc electric field. The figure shows that the bubble diameter decreases as the applied voltage increases. This is physically reasonable because the electric force acting on bubbles increases by increasing the electric field. The calculation shows generally good agreement with measured values. Actual measured diameters are greater than those predicted using a force balance. The uncertainties in bubble volume measurements are estimated to be within about $\pm 10\%$.

Figure 13 shows the relationship between the bubble diameter and the bubble number in the nonuniform electric field. The distribution of bubble diameter without an electric field is wide ($\sim$1.7 mm). In a nonuniform electric field case, it is narrow ($\sim$1.3 mm for 10 kV dc voltage and $\sim$0.9 mm for 20 kV dc voltage). With increasing applied voltage the number of bubbles increases markedly (43 ea for 0 kV, 164 ea for 10 kV dc voltage and 273 ea for 20 kV dc voltage). From these figures, we can see that the distribution of the bubble diameter and number in the electric field is quite different with that in the zero electric field.

3.3.5. Latent heat flux to total heat flux

In the present study, the total heat flux of the wire is composed of two different mechanisms of heat transfer: convection and latent heat. For saturated nucleate boiling, the latent heat transported by bubbles is significant. The latent heat component q_{LH} can be determined by

$$q_{LH} = \frac{1}{\pi D_w} S \times f \times J, \tag{10}$$

where, D_w, S, f and J are the wire diameter, the average nucleation site density, the average bubble frequency and the average heat transport per bubble.

The average heat transport per bubble J can be calculated by

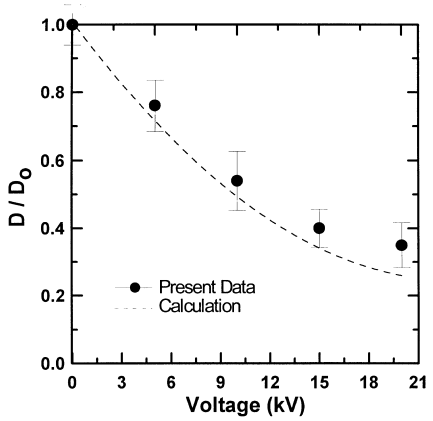

Fig. 12. Average departure diameter of bubbles in a nonuniform dc electric field.

$$J = \frac{\pi}{6}\rho_g h_{fg} D^3, \tag{11}$$

where, ρ_g, h_{fg} and D are the gas density, the latent heat and the equivalent bubble diameter.

Equations (10) and (11) are used to determine how the relative latent heat contribution is changed by a nonuniform electric field. In order to determine the latent heat transport contribution to the heat flux, the average density of active nucleation sites, the average bubble departure frequency, and the average heat transported by a bubble are substituted into Eq. (10).

Figure 14 shows the relative contribution of the convection heat flux, the latent heat flux and the enhanced latent heat flux to the total heat flux. In the absence of an applied voltage, the normal latent heat flux is estimated as about 43% of the total heat flux. With increasing the

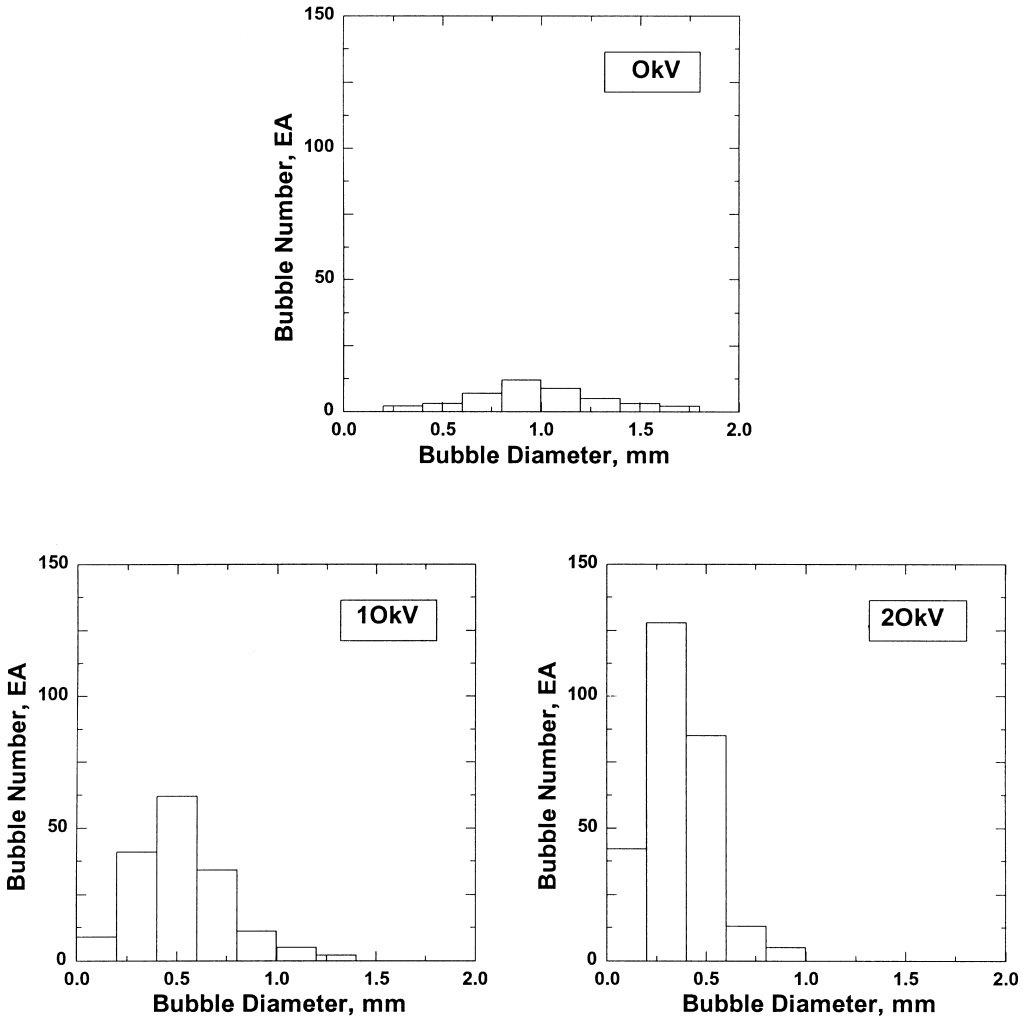

Fig. 13. Relationship between bubble number and bubble diameter in a nonuniform dc electric field.

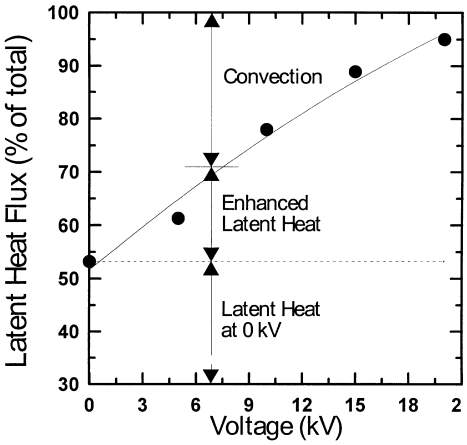

Fig. 14. Relative contribution of convection, latent heat and enhanced latent heat to total heat flux in a nonuniform dc electric field.

applied voltage, the latent heat increases due to the active bubble dynamics. For 20 kV dc voltage, the amount of heat transferred by the convection is small, and then the latent heat transported by bubbles corresponds to the total heat flux. This is due to more active nucleation and the higher bubble frequency, so that great agitation and mixing around the heated wire can be expected. Thus, we can see that the modified EHD phenomena on bubble behavior are effective heat removal mechanism during pool boiling process.

4. Conclusions

In order to investigate the effects of an electric field on the nucleate boiling heat transfer enhancement including bubble dynamic behavior, basic experiments have been performed under saturated pool boiling. Based on the present experimental studies, the following conclusions are obtained.

The experimental results show the shift of the boiling curve, the delay of ONB and CHF to a higher heat flux, and the change of bubble dynamics with increasing the applied voltage. It is found that the electroconvection flow and the EHD boiling effect due to bubble behaviors are responsible for the enhanced heat transfer. The EHD effects are much more remarkable with increasing the applied voltage. Visual observations show that the EHD nucleate boiling enhancement is closely connected with the modified bubble behaviors. The bubble departure cycle is drastically changed by applying a nonuniform electric field. With increasing the applied voltage the active nucleation site density, bubble frequency and bubble velocity increase and the bubble size decreases. It is supposed that the bubble dynamics is very important at pool boiling phenomena under an electric field and dependent strongly on an electric field. At very high voltage, the amount of latent heat transported by bubbles nearly corresponds to the total heat flux. This tendency becomes more prominent for high voltage due to active dynamic behavior of bubbles by EHD effects.

Acknowledgements

The authors wish to thank for referees for their valuable suggestions and comments. This work was supported by an assistance from the Advanced Fluids Engineering Research Center at Pohang University of Science & Technology and the RRC for Advanced Climate Control Technology at Sun Moon University.

References

ASHRAE, 1993. ASHRAE handbook: Fundamental. American Society of Heating, Refrigerating and Air-Conditioning Engineers, Inc.

Carrica, P., Di Marco, P., Grassi, W., 1995. Nucleate pool boiling in the presence of an electric field: effect of subcooling and heat-up rate. In: Symp. Two-phase Flow Modeling and Experimentation, Vol. 2, pp. 1091–1097.

Cho, H.J., Kang, I.S., Kweon, Y.C., Kim, M.H., 1996. Study on the behavior of a bubble attached to the wall in a uniform electric field. Int. J. Multiphase Flow 22, 909–922.

Cho, H.J., Kang, I.S., Kweon, Y.C., Kim, M.H., 1998. Numerical study on the behavior of a bubble attached to a tip in a nonuniform electric field. Int. J. Multiphase Flow 24, 479–498.

Choi, H.Y., 1962. Electrohydrodynamic boiling heat transfer. Ph.D. thesis, Mech. Engineering Dept., MIT.

Cooper, P., 1990. EHD enhancement of nucleate boiling. Trans. ASME 112, 458–464.

Damianidis, C., Karayiannis, T.G., Al-Dadah, P.K., James, R.W., Collins, M.W., Allen, P.H.G., 1992. EHD boiling enhancement in shell-and-tube evaporators and its application in refrigeration plants. In: ASHRAE Trans. Symp., BA-92-5-5, pp. 462–472.

Jones, T.B., 1978. Electrohydrodynamically enhanced heat transfer in liquids: a review. Adv. Heat Transfer 14, 107–148.

Kawahira, H., Kubo, J., Yokoyama, T., Ogata, J., 1990. The effect of an electric field on boiling heat transfer of refrigerant-11-boiling on a single tube. IEEE Trans. Ind. App. 26, 359–365.

Kweon, Y.C., Kim, M.H., Cho, H.J., Kang, I.S., Kim, S.J., 1996. Effects of an electric field on the nucleate pool boiling and bubble behavior on a horizontal wire. In: Chen, J.C. (Ed.), Convective Flow Boiling. Taylor & Francis, pp. 351–356.

Kweon, Y.C., Kim, M.H., Cho, H.J., Kang, I.S., 1998. Study on the deformation and departure of a bubble attached to a wall in dc/ac electric fields. Int. J. Multiphase Flow 24, 145–162.

Kraus, J.D., 1992. Electromagnetics. McGraw-Hill, Inc, New York.

Lovenguth, R.F., 1968. Boiling heat transfer in the presence of electric fields Ph.D. thesis, Department Chemical Engineering, Newark, NJ.

Melcher, J.R., 1981. Continuum Electromechanics. MIT Press.

Moffat, R.J., 1985. Using uncertainty analysis in the planning of an experiment. J. Fluid Eng. 107, 173–182.

Ogata, J., Iwafui, Y., Shimada, Y., Yamazaki, T., 1992. Boiling heat transfer enhancement in tube - bundle evaporators utilizing electric field effects. In: ASHRAE Trans. Symp., BA-92-5-2, pp. 435–444.

Ogata, J., Yabe, A., 1993. Basic study on the enhancement of nucleate boiling heat transfer by applying electric fields. Int. J. Heat Mass Transfer 36, 775–782.

Panofsky, W., Phillips, M., 1962. Classical electricity and magnetism. Addison-Wesley, New York.

Pohl, H.A., 1958. Some effects of nonuniform fields on dielectrics. J. Appl. Phys. 29, 1182.

Seyed-Yagoobi, J., Geppert, C.A., Geppert, L.M., 1996. Electrohydro-dynamically enhanced heat transfer in pool boiling. Journal of Heat Transfer 118, 233–237.

Turnbull, R.J., 1968. Electroconvective instability with a stabilizing temperature gradient. I. Theory. Phys. Fluids 11, 2597–2603.

Turnbull, R.J., 1968. Electroconvective instability with a stabilizing temperature gradient. II. Experimental results. Phys. Fluids 11, 2597–2603.

Wang, T., Simon, T.W., 1988. Development of a special-purpose test surface guided by uncertainty analysis: Introduction of a new uncertainty analysis step. AIAA 26th Aerospace Sciences Meeting, pp.1–9.

Yabe, A., Maki, H., 1988. Augmentation of convective and boiling heat transfer by applying an electrohydrodynamical liquid jet. Int. J. Heat Mass Transfer 31, 407–417.